

# Covariant Density Functional Theory in Nuclear Physics and Astrophysics

Junjie Yang and J. Piekarewicz

Department of Physics, Florida State University, Tallahassee, FL 32306-4350, U.S.A; email: jpiekarewicz@fsu.edu

Xxxx. Xxx. Xxx. Xxx. YYYY. AA:1–24

[https://doi.org/10.1146/\(\(please add article doi\)\)](https://doi.org/10.1146/((please add article doi)))

Copyright © YYYY by Annual Reviews.  
All rights reserved

## Keywords

density functional theory, equation of state, neutron stars

## Abstract

*How does subatomic matter organize itself?* Neutron stars are cosmic laboratories uniquely poised to answer this fundamental question that lies at the heart of nuclear science. Newly commissioned rare isotope facilities, telescopes operating across the entire electromagnetic spectrum, and ever more sensitive gravitational wave detectors will probe the properties of neutron-rich matter with unprecedented precision over an enormous range of densities. Yet, a coordinated effort between observation, experiment, and theoretical research is of paramount importance for realizing the full potential of these investments. Theoretical nuclear physics provides valuable insights into the properties of neutron-rich matter in regimes that are not presently accessible to experiment or observation. In particular, nuclear density functional theory is likely the only tractable framework that can bridge the entire nuclear landscape by connecting finite nuclei to neutron stars. This compelling connection is the main scope of the present review.

## Contents

1. INTRODUCTION .....	2
2. FORMALISM .....	5
2.1. Covariant Density Functional Theory .....	5
2.2. Neutron Stars .....	9
2.3. Equation of State .....	11
3. RESULTS .....	13
3.1. Ground State Properties .....	13
3.2. Neutron Star Properties .....	13
4. CONCLUSIONS .....	19

## 1. INTRODUCTION

Nuclear science is poised to enter a period of transformational changes driven by the upgrade and commissioning of state-of-the-art experimental and observational facilities. As we embark on this new journey of discovery, nuclear theory will play a critical role in guiding new experimental programs and in predicting the properties of nuclear matter in regimes that will remain inaccessible to experiment and observation. With unparalleled depth and breadth, nuclear science is driven by the quest to answer fundamental questions ranging from the quark-gluon structure of hadronic matter to the synthesis of heavy elements in cataclysmic stellar explosions (1). In this contribution we focus on the critical role that Density Functional Theory (DFT) plays in our understanding of a variety of nuclear phenomena that range from the structure and dynamics of exotic nuclei to the fascinating properties of neutron stars. Remarkable advances in theoretical nuclear physics have propelled traditional wave function methods to such heights that highly accurate predictions of the properties of small to medium size nuclei are now routine; see Refs. (2, 3, 4, 5) and references contained therein. Such “ab initio” approaches provide meaningful benchmarks for the development of reliable energy density functionals which can then be applied to larger nuclear systems. Indeed, this powerful connection between ab initio approaches and DFT is one of the main motivations behind the  $^{48}\text{Ca}$  Radius EXperiment (CREX) at Jefferson Lab (6, 7). Multiple paths exist for improving the performance of nuclear energy density functionals and on transforming them into proper effective field theories. For a recent perspective on how to approach this challenging task see Ref. (8) and references contained therein.

Density Functional Theory is a powerful technique developed by Kohn and collaborators (9, 10) in the mid 60s to understand the electronic structure of complex many-body systems and for which Kohn was recognized with the 1998 Nobel Prize in Chemistry (11). Today, DFT is widely used in chemistry as well as in many areas of physics (12, 13, 14, 15). In its original application to electronic structure, Hohenberg and Kohn (HK) assumed the validity of the Born-Oppenheimer approximation, which defines the many-body Hamiltonian in terms of a conventional kinetic-energy contribution, a two-body potential that accounts for the electronic repulsion, and a one-body attractive potential provided by the “stationary” nuclei. Given that in the Born-Oppenheimer approximation the position of the heavy nucleus is assumed to be fixed, this last term is commonly referred to as the *exter-*

that a one-to-one correspondence exists between the one-body electronic density and a suitable external potential and (b) that an energy density functional (EDF) exists which upon functional minimization yields both the exact ground-state energy and one-body density of the complicated many-body system (9). Essentially, the HK theorems establish a remarkable and subtle result, namely, that the exact ground-state energy of the complicated many-body system may be obtained from minimizing a *suitable* EDF that only depends on the one-body density. Perhaps the greatest virtue of DFT is that it shifts the focus from the complicated many-body wave function that depends on  $3N$  spatial coordinates (for an  $N$ -particle system) to the much more intuitive one-body density that depends only on three. By doing so, DFT not only reduces drastically the complexity of the problem, but also invites physical insights into the construction of the functional. This is particularly relevant given that the HK theorem is an *existence* theorem that offers no guidance on how to construct the appropriate energy density functional. This presents a serious challenge to the implementation, as no accurate representation of the kinetic energy part of the EDF exists.

In an effort to mitigate this problem and inspired by Hartree-Fock theory, Kohn and Sham replaced the complex interacting system by an equivalent system of *non-interacting* electrons moving in a suitably-generated external potential (10). The term “equivalent” is used to indicate that the Kohn-Sham (KS) potential must be sophisticated enough to reproduce the exact one-body density of the interacting system. So while the KS equations for the fictitious system closely resemble the structure of the Hartree equations, they differ by the presence of an *exchange correlation* term that ensures that its density is identical to that of the interacting system. In essence, the KS approach trades the search for an accurate energy density functional for that of a complex exchange correlation potential. Nevertheless, the reformulation of the DFT problem in terms of one-particle orbitals has several advantages. First, unlike “orbital-free” DFT where the kinetic-energy functional is unknown and complex, the kinetic energy term for the fictitious system is known. Second, the computational cost is minimal as it increases linearly with the number of occupied orbitals. Third, the construction of the one-body density involves a simple sum over the occupied single-particle orbitals. Finally, self-consistent problems of this kind have been around for almost a century, so efficient and robust methods for their solution abound. Note that self-consistency is demanded because the one-body density depends on the single-particle orbitals which, in turn, are solutions of a Schrödinger (or Dirac) equation in the presence of a density-dependent KS potential.

After this historical interlude it is appropriate to ask how can DFT be extended from the electronic sector to the nuclear domain. Unfortunately, the answer is far from obvious (8). One immediate difficulty concerns the one-to-one correspondence between the one-body density and the external potential, a concept that lies at the heart of DFT. As a self-bound, many-body system, atomic nuclei are not subjected to any external potential. Hence, within the scope of the original “orbital-free” DFT of Hohenberg and Kohn (9), the generalization to nuclear physics is unclear. Yet, within the “mean-field like” Kohn-Sham paradigm some similarities emerge. After all, mean-field theory has been an integral part of nuclear theory for many decades; see Ref. (16) and references contained therein. Although the external potential is germane to the KS formalism, could one simply regard the nuclear mean field as the KS potential without the all important external potential? Regretfully, this is not the case, mainly because of the necessity of the complicated *exchange-correlation* potential that is essential to reproduce the exact ground state energy. Indeed, neglecting the

exchange correlation potential reduces the KS equations to the much simpler set of Hartree equations (11). However, in the context of nuclear physics it is well known that a Hartree potential computed from the convolution of the “bare” nucleon-nucleon interaction with the nuclear density provides a poor description of the properties of atomic nuclei (16). To overcome this problem “effective density dependent forces” were developed by Skyrme almost a decade before the inception of density functional theory (17, 18). In particular, part of the success of the Skyrme interaction relies on the existence of powerful relations connecting the (isoscalar) parameters of the model to various bulk properties of infinite nuclear matter, such as the saturation density, binding energy per nucleon, and incompressibility coefficient (19, 20). In this manner important features of the nuclear dynamics are directly encoded into the parameters of the model. Reminiscent of the Hartree-Fock—or the more modern Kohn-Sham approach—the resulting single-particle equations of motion are derived from functional minimization of a properly defined Skyrme energy density functional. So while the notion of a nuclear mean-field potential remains essential, its connection to the underlying (or “bare”) nucleon-nucleon interaction has been lost. Indeed, present day nuclear EDFs are largely empirical, as the parameters of the model have no direct connection to the underlying nucleon-nucleon interaction often calibrated using deuteron properties and phase shifts. Rather, in DFT the model parameters are fitted to selected properties of atomic nuclei. One often justifies empirical EDFs by invoking the HK theorems, which as existence theorems provide no guidance on how to construct the functional. Nevertheless, significant advances have been made over the last decade to mitigate the reliance on empirical EDFs in favor of more fundamental ones; for an extensive reviews entitled *Toward ab initio density functional theory for nuclei* see Ref. (15) and references contain therein. In parallel, much effort has also been devoted to the construction of a *Universal Nuclear Energy Density Functional* with the aim of achieving a comprehensive understanding of finite nuclei across the entire nuclear landscape (21, 22, 23, 24, 25).

In this review we will continue to rely on empirical EDFs, but within the context of *covariant density functional theory*. Our motivation for this generalization is mostly pragmatical, as we seek a unified approach that can simultaneously describe the dynamics of finite nuclei and neutron stars, systems with natural length scales that differ by 18 orders of magnitude! We aim to build high-quality functionals that yield an accurate description of the properties of finite nuclei, generate an equation of state that is consistent with known neutron-star properties, while providing a Lorentz covariant extrapolation to dense matter. In the case of finite nuclei, an important goal is not only to compute ground state properties, but also the linear response of the ground state to a variety of probes. In this context DFT continues to provide an ideal framework. Indeed, given the variational nature of DFT, small oscillations around the variational minimum encapsulate the linear response of the ground state to weak external perturbations. However, care must be exercised in employing a residual interaction that is consistent with the one employed to generate the ground state. Only then can one ensure that important symmetries and conservation laws are properly enforced (26, 27, 28, 29). Finally, given that some of the observables of interest require extrapolations into regions that are inaccessible in the laboratory, we aim when possible to supplement our predictions with theoretical uncertainties (23, 30, 31, 30, 32, 33, 34, 35, 36, 37). This can now be done routinely as the calibration of the EDF produces a statistically robust covariant matrix.

Exploring the synergy between nuclear physics and astrophysics has always been a core mission of nuclear science. In the particular context of neutron stars, the equation

of state prescribed by the underlying DFT becomes essential in the description of the structure and dynamics of these fascinating compact objects. The powerful connection between nuclear physics and astrophysics has just been strengthened even further with the first direct detection of gravitational waves from the binary neutron star merger GW170817 (38). In one clean sweep GW170817 has confirmed the long-held belief that short gamma ray bursts are associated with the merger of two neutron stars; has identified the left-over *kilonova* as the electromagnetic transient powered by the radioactive decay of the heavy elements synthesized in the rapid neutron-capture process (39, 40, 41, 42); and has provided stringent constraints on the equation of state (43, 44, 45, 46, 47, 48, 49, 50, 51). Assessing the impact of this historic discovery will be an important component of this review.

We have organized the review as follows. In Sec. 2 we start by discussing the class of covariant density functionals that will be considered in this work. We then introduce the associated set of equations that must be solved to obtain Kohn-Sham orbitals and ground-state densities. We then proceed to illustrate, also in Sec. 2, how to compute the nuclear matter equation of state using the same exact covariant EDFs. Note that the EOS is the sole ingredient required to solve the equations of hydrostatic equilibrium from which several neutron-star properties are extracted. Having developed the formalism, we then move to Sec. 3 where our predictions are discussed, with special emphasis on those observables that are difficult to probe under present laboratory conditions, either because of the large neutron excess or the very high density. We conclude and offer our perspectives for the future in Sec. 4.

## 2. FORMALISM

In this section we develop the formalism underpinning covariant density functional theory and focus on its implementation to the physics of finite nuclei and neutron stars. The Dirac equation obeyed by the nucleon fields and the associated Klein-Gordon equations for the meson fields may be regarded as the generalization of the Kohn-Sham equations to the domain of covariant DFT. Note that as alluded earlier, the effective interaction bears little resemblance to the underlying nucleon-nucleon interaction, as the parameters of the model are calibrated to the properties of finite nuclei rather than to two-nucleon data. The application to neutron stars relies on the same energy density functional without any adjustments. That is, the equation of state that serves as the sole input for the Tolman-Oppenheimer-Volkoff equations is constructed from the same model used to compute the properties of finite nuclei, thereby connecting problems with length scales that differ by about 18 orders of magnitude. Because of space limitations, we omit discussing the collective nuclear response, an interesting area of investigation that will continue to thrive with the advent of radioactive beam facilities. For a review of collective excitations in the context of covariant DFT see Refs. (52, 53) and references contained therein.

### 2.1. Covariant Density Functional Theory

Finite nuclei are complex many-body systems governed largely by the strong nuclear force. Although quantum chromodynamics (QCD) is the fundamental theory of the strong interaction, many technical hurdles still prevent us from applying QCD in the non-perturbative regime of relevance to nuclear physics. To date, density functional theory is the most

nuclear landscape: from finite nuclei to neutron stars. In the traditional non-relativistic approach, the dynamical information is encoded in an effective interaction between nucleons that is used to build the energy density functional in terms of conserved isoscalar and isovector (or proton and neutron) densities and their associated currents (21, 22). The paradigm of such an effective non-relativistic interaction is the Skyrme interaction (17, 18, 19, 20). Given that the model parameters cannot be computed from first principles, various optimization protocols are being used to adjust their values by fitting to a suitable set of experimental data (23, 24, 25). From such an optimally calibrated density functional, one derives the corresponding Kohn-Sham equations which are then solved using self-consistent mean-field methods (54)

Covariant density functional theory follows in the footsteps of Skyrme DFT, but with both nucleons and mesons as the fundamental degrees of freedom. Among the earliest attempts at a relativistic description of the nuclear dynamics is the work of Johnson and Teller (55), Duerr (56), and Miller and Green (57); for a more complete historical account see Ref. (58). Besides a desire to understand the saturation of nuclear matter and its impact on the ground-state energy and densities of atomic nuclei, an important motivation for a relativistic description—and one that remains true to this day—was the development of a theory of highly condensed matter that could be applied to the study of neutron stars (59). Originally, Quantum Hadrodynamics (or QHD) was conceived as a quantum field theory consisting of a nucleon field interacting via the exchange of neutral scalar and vector mesons (59). Remarkably, a self-consistently generated equation of state for symmetric nuclear matter exhibits saturation—even at the mean field level—because of the different Lorentz character of the scalar and vector interactions. Moreover, pure neutron matter was found to be unbound and to remain causal at all densities. However, whereas nuclear saturation—the existence of an equilibrium density at which the pressure vanishes—represented a great triumph of the theory, the curvature around the minimum, *i.e.*, the incompressibility coefficient, was inconsistent with experimental limits obtained from the measurement of the monopole response of heavy nuclei (60). To remedy this deficiency, scalar-meson self interactions, first introduced by Boguta and Bodmer (61), were successful in softening the equation of state. Since then, modifications to the underlying effective Lagrangian density were introduced in an effort to provide a more accurate description of the properties of finite nuclei and neutron stars (37, 58, 62, 63, 64, 65, 66, 67, 68, 69). Moreover, some of the most recent parametrizations now provide properly quantified statistical uncertainties.

In the framework of covariant DFT, the basic degrees of freedom are the nucleon (protons and neutrons), three mesons, and the photon. The isodoublet nucleon field  $\psi$  interacts via the exchange of photons ( $A_\mu$ ) as well as three massive “mesons”: the isoscalar-scalar  $\sigma$  meson, the isoscalar-vector  $\omega$  meson, and the isovector-vector  $\rho$  meson (58, 59, 70). The effective (interacting) Lagrangian density takes the following form (58, 62, 71, 72),

$$\begin{aligned}
\mathcal{L}_{\text{int}} &= \bar{\psi} \left[ g_s \phi - \left( g_v V_\mu + \frac{g_\rho}{2} \boldsymbol{\tau} \cdot \mathbf{b}_\mu + \frac{e}{2} (1 + \tau_3) A_\mu \right) \gamma^\mu \right] \psi \\
&\quad - \frac{\kappa}{3!} (g_s \phi)^3 - \frac{\lambda}{4!} (g_s \phi)^4 + \frac{\zeta}{4!} g_v^4 (V_\mu V^\mu)^2 + \Lambda_v \left( g_\rho^2 \mathbf{b}_\mu \cdot \mathbf{b}^\mu \right) \left( g_v^2 V_\nu V^\nu \right) \\
&\equiv \bar{\psi} \left[ g_s \phi - \left( g_v V_\mu + \frac{g_\rho}{2} \boldsymbol{\tau} \cdot \mathbf{b}_\mu + \frac{e}{2} (1 + \tau_3) A_\mu \right) \gamma^\mu \right] \psi - U_{\text{eff}}(\phi, V_\mu, \mathbf{b}_\mu). \quad 1.
\end{aligned}$$

The first line in the above equation contains the conventional meson-nucleon Yukawa couplings, while the second line contains the self-interactions. Here ( $\mathbf{b}_\mu$ ) is the

serve to simulate the complicated many-body dynamics and that are required to improve the predictive power of the model. As already alluded, the two isoscalar parameters  $\kappa$  and  $\lambda$  introduced by Boguta and Bodmer (61) were designed to reduce the incompressibility coefficient of symmetric nuclear matter in accordance to measurements of giant monopole resonances in finite nuclei (60). Sometime later, Müller and Serot introduced the isoscalar parameter  $\zeta$  to soften the equation of symmetric nuclear matter but at much higher densities (62). Indeed, they found that by tuning the value of  $\zeta$  one could significantly modify the maximum neutron star mass without compromising the success of the model in reproducing ground-state observables. Finally, the mixed isoscalar-isovector parameter  $\Lambda_\nu$  was introduced to modify the density dependence of the symmetry energy—particularly its slope at saturation density  $L$ . The structure of both neutron-rich nuclei and neutron stars is highly sensitive to the slope of the symmetry energy (71, 73, 74).

The field equations resulting from the above Lagrangian density may be solved exactly in the mean-field limit, where the meson-field operators are replaced by their classical expectation values (58, 59). For a static and spherically symmetric ground state this implies:

$$\phi(x) \rightarrow \langle \phi(x) \rangle = \phi_0(r), \quad 2a.$$

$$V^\mu(x) \rightarrow \langle V^\mu(x) \rangle = g^{\mu 0} V_0(r), \quad 2b.$$

$$b_a^\mu(x) \rightarrow \langle b_a^\mu(x) \rangle = g^{\mu 0} \delta_{a3} b_0(r), \quad 2c.$$

$$A^\mu(x) \rightarrow \langle A^\mu(x) \rangle = g^{\mu 0} A_0(r). \quad 2d.$$

Given that the meson fields couple to their associated bilinear nucleon currents, the baryon sources must also be replaced by their (normal-ordered) expectation values in the mean-field ground state:

$$\bar{\psi}(x)\psi(x) \rightarrow \langle : \bar{\psi}(x)\psi(x) : \rangle = \rho_s(r), \quad 3a.$$

$$\bar{\psi}(x)\gamma^\mu\psi(x) \rightarrow \langle : \bar{\psi}(x)\gamma^\mu\psi(x) : \rangle = g^{\mu 0} \rho_\nu(r), \quad 3b.$$

$$\bar{\psi}(x)\gamma^\mu\tau_a\psi(x) \rightarrow \langle : \bar{\psi}(x)\gamma^\mu\tau_a\psi(x) : \rangle = g^{\mu 0} \delta_{a3} \rho_3(r), \quad 3c.$$

$$\bar{\psi}(x)\gamma^\mu\tau_p\psi(x) \rightarrow \langle : \bar{\psi}(x)\gamma^\mu\tau_p\psi(x) : \rangle = g^{\mu 0} \rho_p(r), \quad 3d.$$

where  $\rho_s$  is the dynamically generated scalar density,  $\rho_\nu$  the conserved isoscalar baryon density,  $\rho_3$  the isovector baryon density, and  $\rho_p$  the proton density. In terms of the individual proton and neutron densities, one can write  $\rho_\nu = \rho_p + \rho_n$  and  $\rho_3 = \rho_p - \rho_n$ . Note that we have introduced the proton isospin projection operator as  $\tau_p = (1 + \tau_3)/2$ . Using the above approximations one can now derive the associated Euler-Lagrangian equations of motion for a generic quantum field  $q_i$  (58):

$$\partial_\mu \left[ \frac{\partial \mathcal{L}}{\partial (\partial_\mu q_i)} \right] - \frac{\partial \mathcal{L}}{\partial q_i} = 0. \quad 4.$$

In the particular case of the Lagrangian density given in Eq.(1), the classical meson field

state baryon densities as source terms. That is,

$$\left(\nabla^2 - m_s^2\right)\phi_0(r) - \frac{\partial U_{\text{eff}}}{\partial \phi_0} = -g_s \rho_s(r), \quad 5a.$$

$$\left(\nabla^2 - m_v^2\right)V_0(r) + \frac{\partial U_{\text{eff}}}{\partial V_0} = -g_v \rho_v(r), \quad 5b.$$

$$\left(\nabla^2 - m_\rho^2\right)b_0(r) + \frac{\partial U_{\text{eff}}}{\partial b_0} = -\frac{g_\rho}{2} \rho_3(r). \quad 5c.$$

In turn, the Coulomb field satisfied the much simpler Poisson's equation:

$$\nabla^2 A_0 = -e\rho_p. \quad 6.$$

On the other hand, the nucleons satisfy a Dirac equation with the meson fields generating scalar and time-like vector mean-field potentials. That is,

$$\left[-i\boldsymbol{\alpha} \cdot \boldsymbol{\nabla} + g_v V_0(r) + \frac{g_\rho}{2} \tau_3 b_0(r) + e\tau_p A_0(r) + \beta(M - g_s \phi_0(r))\right] \psi(\mathbf{r}) = E\psi(\mathbf{r}). \quad 7.$$

The above set of equations—Eqs.(5-7)—represent the effective Kohn-Sham equations for the nuclear many-body problem. As such, this set of mean-field equations must be solved self-consistently. That is, the single-particle orbitals satisfying the Dirac equation are generated from the various meson fields which, in turn, satisfy Klein-Gordon equations with the appropriate ground-state densities as the source terms. This demands an iterative procedure in which mean-field potentials of the Wood-Saxon form are initially provided to solve the Dirac equation for the occupied nucleon orbitals which are then combined to generate the appropriate densities for the meson field. The Klein-Gordon equations are then solved with the resulting meson fields providing a refinement to the initial mean-field potentials. This procedure continues until self-consistency is achieved; see Ref.(72) for a detailed description on the implementation. Due to the highly non-linear structure of these equations, extra care must be exercised in ensuring that self-consistency has indeed been achieved.

In the spirit of covariant DFT, the outcome of the iterative procedure are ground-state densities, binding energies, and self-consistent mean fields. However, given the empirical nature of the covariant DFT, one must first adjust the parameters of the interacting density given in Eq.(1) to available experimental/observational data. Recently, such calibrating procedure has been implemented without any reliance on “pseudo-data”, namely without incorporating assumed bulk properties of infinite nuclear matter (37, 69). Moreover, besides predicting (rather than assuming) the values of several bulk properties of nuclear matter, the statistical approach adopted in the calibrating procedure allows one to provide quantifiable theoretical errors. In doing so, one discovers that the isoscalar sector of the density functional, namely, the sector that does not distinguish neutrons from protons, is fairly well constrained by existing nuclear observables. This is not surprising as most of the experimental nuclear observables available today probe small to moderate neutron-proton asymmetries. In contrast, the isovector sector of the nuclear density functional is poorly constrained. As it stands now, the two isovector parameters defining the effective Lagrangian density in Eq.(1) are the Yukawa coupling  $g_\rho$  and the mixed isoscalar-isovector coupling  $\Lambda_v$ . As shown in Ref. (37), these two model parameters can be fixed once two fundamental parameters of the nuclear symmetry energy are inferred; see Sec.2.3. Enormous theoretical and experimental efforts have been devoted for the last two decades to constrain these two parameters, or more generally the density dependence of the nuclear symmetry energy. Progress towards achieving this goal by using both laboratory data and

## 2.2. Neutron Stars

Having explained the main features of the covariant DFT formalism, we are now in a position to examine the structure of neutron stars. The structure of spherically symmetric neutron stars in hydrostatic equilibrium—in particular the fundamental mass-vs-radius relation—is encapsulated in the Tolman-Oppenheimer-Volkoff (TOV) equations (75, 76). Adopting natural units in which  $G=c=1$ , the TOV equations are given by

$$\frac{dP(r)}{dr} = - \frac{(\varepsilon(r) + P(r)) (M(r) + 4\pi r^3 P(r))}{r^2 (1 - 2M(r)/r)}, \quad 8a.$$

$$\frac{dM(r)}{dr} = 4\pi r^2 \varepsilon(r). \quad 8b.$$

Here  $M(r)$ ,  $P(r)$ ,  $\varepsilon(r)$  represent the enclosed mass, pressure, and energy density profiles, respectively. The TOV equations represent the extension of Newtonian gravity to the domain of general relativity. Such extension is essential as the typical escape velocity from the surface of neutron star is close to the speed of light. Indeed, the Schwarzschild radius of a neutron star (of the order of 3-6 kilometers) is comparable to its 12-14 kilometer radius. That is,

$$\frac{v_{\text{esc}}^2}{c^2} = \frac{2GM}{c^2 R} \equiv \frac{R_s(M)}{R}. \quad 9.$$

Upon inspection, one notices that the only input required for the solution of the TOV equations is an equation of state, namely, a relation between the pressure and the energy density. Providing such an EOS is within the purview of nuclear physics. Although unknown to Oppenheimer and Volkoff at the time of their original contribution (76), the main reason that nuclear physics plays such a predominant role is easy to understand. Back in 1939 Oppenheimer and Volkoff concluded that a neutron star supported exclusively by the quantum pressure from its degenerate neutrons will collapse once its mass exceeds  $0.7 M_\odot$ . Today, however, the evidence for significantly more massive neutron stars is overwhelming (77, 78). Indeed, within the last decade the existence of three neutron stars with masses in the vicinity of  $2M_\odot$  has been firmly established (79, 80, 81). In fact, the most massive neutron star observed to date ( $M = 2.1_{-0.09}^{+0.10} M_\odot$ ) was reported very recently by Cromartie and collaborators (81). This implies that the additional support against gravitational collapse must come from nuclear interactions, which at the high densities (or short distances) of the stellar core are known to be strongly repulsive. The large discrepancy between recent observations and the 80-year old prediction by Oppenheimer and Volkoff has effectively transferred ownership of the neutron-star problem to nuclear physics. It is appropriate to mention that unlike the well-known collapse of a white-dwarf star, the existence of a maximum neutron-star mass is a purely general-relativistic effect with no counterpart in Newtonian gravity. Whereas the collapse of a white-dwarf star is characterized by a dramatic reduction in the stellar radius as the mass approaches the Chandrasekhar limit of  $M_{\text{Ch}} = 1.4 M_\odot$  (82), the existence of a maximum neutron-star mass develops as an instability against small radial perturbations (83). The maximum neutron-star mass is presently unknown, although it has been suggested that GW170817 already provides some important constraints (84).

The existence of neutron stars with masses in excess of  $2M_\odot$  demands a “stiff” equation of state, namely, one in which the pressure increases rapidly with energy density. In contrast, the recent detection of gravitational waves from the binary neutron star merger GW170817

the extraction of a rather small value for the tidal deformability (or polarizability) of a  $M = 1.4 M_\odot$  neutron star (38, 46). The dimensionless tidal deformability is defined as

$$\Lambda = \frac{2}{3} k_2 \left( \frac{c^2 R}{GM} \right)^5 = \frac{64}{3} k_2 \left( \frac{R}{R_s} \right)^5, \quad 10.$$

where  $k_2$  is known as the second Love number (85, 86). Clearly,  $\Lambda$  is extremely sensitive to the compactness parameter  $\xi \equiv R_s/R$  (87, 88, 89, 90, 91, 92, 93). Given that  $k_2$  is known to display a mild sensitivity to the underlying equation of state (93), a measurement of  $\Lambda$ , for a given mass, determines the stellar radius and ultimately the stiffness of the equation of state.

Trying to account for both large masses and small radii creates an interesting tension that once resolved is bound to provide fundamental insights into the EOS. One possibility is that the equation of state is relatively soft at about twice nuclear matter saturation density, which is the region believed to be most strongly correlated to the stellar radius (94). In this density domain the stellar radius is primarily controlled by the density dependence of the nuclear symmetry energy (32, 37, 71, 73, 74). On the other hand, the maximum stellar mass is controlled by the equation of state at the highest densities. Thus, one may be able to account for both large masses and small radii if the equation of state is soft at intermediate densities and then stiffens at higher densities. Insights into the behavior of the symmetry energy can be gleaned from the recently completed (and currently being analyzed) PREX-II measurement of the neutron skin thickness of  $^{208}\text{Pb}$  at the Jefferson Laboratory. It has been demonstrated that the neutron skin thickness of  $^{208}\text{Pb}$  is strongly correlated to the slope of the nuclear symmetry energy at saturation density (95, 96, 97, 98).

Having established the importance of the tidal polarizability in elucidating the structure of neutron stars, we conclude this section with a brief description of the necessary steps involved in its computation. For simplicity, one can assume that mass, pressure, and energy density profiles are available after having solved the TOV equations, leaving the second Love number  $k_2$  (85, 86) as the only unknown parameter appearing in Eq. (10). Evidently,  $\Lambda$  is extremely sensitive to the compactness parameter  $\xi$  (87, 88, 89, 90, 91, 92). In turn, the second Love number  $k_2$  depends on both  $\xi$  and  $y_R$ ,

$$\begin{aligned} k_2(\xi, y_R) = & \frac{1}{20} \xi^5 (1 - \xi)^2 \left[ (2 - y_R) + (y_R - 1) \xi \right] \\ & \times \left\{ \left[ (6 - 3y_R) + \frac{3}{2} (5y_R - 8) \xi \right] \xi + \frac{1}{2} \left[ (13 - 11y_R) + \frac{1}{2} (3y_R - 2) \xi + \frac{1}{2} (1 + y_R) \xi^2 \right] \xi^3 \right. \\ & \left. + 3 \left[ (2 - y_R) + (y_R - 1) \xi \right] (1 - \xi)^2 \ln(1 - \xi) \right\}^{-1}, \quad 11. \end{aligned}$$

where  $y_R \equiv y(r = R)$  is obtained after solving the following non-linear, first order differential equation for  $y(r)$ —a quantity that is closely related to the tidally-induced quadrupole field (90, 91, 93). That is,

$$r \frac{dy(r)}{dr} + y^2(r) + F(r)y(r) + r^2 Q(r) = 0, \quad \text{with } y(0) = 2. \quad 12.$$

density profiles of the star:

$$F(r) = \frac{1 - 4\pi r^2 (\varepsilon(r) - P(r))}{\left(1 - \frac{2M(r)}{r}\right)}, \quad 13a.$$

$$Q(r) = \frac{4\pi}{\left(1 - \frac{2M(r)}{r}\right)} \left(5\varepsilon(r) + 9P(r) + \frac{\varepsilon(r) + P(r)}{c_s^2(r)} - \frac{6}{4\pi r^2}\right) - 4 \left[ \frac{\left(M(r) + 4\pi r^3 P(r)\right)}{r^2 \left(1 - \frac{2M(r)}{r}\right)} \right]^2. \quad 13b.$$

Note that in addition  $Q(r)$  depends on the speed of sound profile, which involves the derivative of the pressure with respect to the energy density, *i.e.*,

$$c_s^2(r) = \frac{dP(r)}{d\varepsilon(r)}. \quad 14.$$

A covariant energy density functional—unlike nonrelativistic functionals—ensures that the EOS remains causal at all densities, namely, that the speed of sound never exceeds the speed of light.

### 2.3. Equation of State

Neutron stars are “cold” dense objects with a characteristic core temperature significantly lower than the corresponding Fermi temperature (94, 99). As such, and under the assumption of spherical symmetry and hydrostatic equilibrium, the relevant equation of state is that of a zero temperature, electrically-neutral system in chemical (or “beta”) equilibrium. As we aim to build a covariant energy density functional that describes the properties of both finite nuclei and neutron stars, we adopt as the basic constituents of matter, neutrons, protons, and leptons (both electrons and muons). Note that leptons help maintain both charge neutrality and beta equilibrium, which ultimately sets the proton fraction in the neutron star, a critical property that impacts many stellar properties.

Although beta equilibrium dictates that only the total baryon density is conserved, we start with a discussion of the EOS of infinite nuclear matter where both neutron and proton densities are individually conserved. Infinite nuclear matter is an idealized system of protons and neutrons interacting solely via the strong nuclear force, so that both electromagnetic and weak interactions are “turned off”. In such an idealized situation and under the assumption of translational invariance, the expectation value of the various meson fields in Eq.(5) are uniform (*i.e.*, constant throughout space) and the Kohn-Sham orbitals in Eq.(7) are plane-wave Dirac spinors with medium-modified effective masses and energies that must be determined self-consistently. To derive the equation of state of infinite nuclear matter one invokes the energy-momentum tensor:

$$\mathcal{T}_{\mu\nu} = -g_{\mu\nu}\mathcal{L} + \left[ \frac{\partial\mathcal{L}}{\partial(\partial^\mu q_i)} \right] \partial_\nu q_i, \quad 15.$$

where a sum over all constituent fields  $q_i$  is assumed. For a uniform system such as infinite nuclear matter, the expectation value of the energy momentum tensor takes the following simple form (58):

where  $u^\mu = \gamma(1, \boldsymbol{\beta})$  is the scaled four-velocity of the fluid that satisfies the Lorentz-invariant condition  $u^2 = u^\mu u_\mu = 1$ , with  $\gamma$  being the Lorentz factor. In particular, for infinite nuclear matter at rest, *i.e.*,  $u^\mu = (1, \mathbf{0})$ , it follows that

$$\mathcal{E} = \langle \mathcal{T}_{00} \rangle \text{ and } P = \frac{1}{3} \langle \mathcal{T}_{ii} \rangle. \quad 17.$$

Given that both the proton and neutron densities are conserved in infinite nuclear matter, the equation of state at zero temperature may be written as either a function of the individual densities or as a function of the total baryon density  $\rho = \rho_n + \rho_p$  and the neutron-proton asymmetry  $\alpha \equiv (\rho_n - \rho_p)/(\rho_n + \rho_p)$ . Expanding the energy per nucleon in even powers of the neutron-proton asymmetry is particularly insightful. That is,

$$\frac{E}{A}(\rho, \alpha) - M \equiv \mathcal{E}(\rho, \alpha) = \mathcal{E}_{\text{SNM}}(\rho) + \alpha^2 \mathcal{S}(\rho) + \mathcal{O}(\alpha^4). \quad 18.$$

Here  $\mathcal{E}_{\text{SNM}}(\rho) = \mathcal{E}(\rho, \alpha \equiv 0)$  is the energy per nucleon of symmetric nuclear matter (SNM) and the symmetry energy  $\mathcal{S}(\rho)$  represents the first-order correction to the symmetric limit. Note that no odd powers of  $\alpha$  appear in the expansion since in the absence of electroweak interactions the nuclear force is assumed to be isospin symmetric; isospin violations in the nucleon-nucleon interactions (which are small) are henceforth neglected. Although there is *a priori* no reason to neglect the higher order terms in Eq.(18), for the models considered in this review the symmetry energy represents to a very good approximation the energy cost required to convert symmetric nuclear matter into pure neutron matter (PNM). That is,

$$\mathcal{S}(\rho) \approx \mathcal{E}(\rho, \alpha = 1) - \mathcal{E}(\rho, \alpha = 0). \quad 19.$$

While the above relation is model dependent, its validity is easily verified in the case that protons and neutrons behave as non-interacting Fermi gases (100). The separation of the energy per nucleon as in Eq.(18) is useful because symmetric nuclear matter is sensitive to the isoscalar sector of the density functional which is well constrained by the properties of stable nuclei. In contrast, the symmetry energy probes the isovector sector of the density functional which at present is poorly constrained because of the lack of experimental data on very neutron-rich systems. However, this problem will soon be mitigated with the commissioning of radioactive beam facilities throughout the world.

Besides the separation of the EOS into isoscalar and isovector components, it is also useful to characterize the equation of state in terms of a few of its bulk parameters defined at saturation density. Nuclear saturation, the existence of an equilibrium density that characterizes the interior of medium to heavy nuclei, is a hallmark of the nuclear dynamics. By performing a Taylor series expansion around nuclear matter saturation density  $\rho_0$  one obtains (101):

$$\mathcal{E}_{\text{SNM}}(\rho) = \varepsilon_0 + \frac{1}{2} K_0 x^2 + \dots, \quad 20a.$$

$$\mathcal{S}(\rho) = J + Lx + \frac{1}{2} K_{\text{sym}} x^2 + \dots, \quad 20b.$$

where  $x = (\rho - \rho_0)/3\rho_0$  is a dimensionless parameter that quantifies the deviations of the density from its value at saturation. Here  $\varepsilon_0$  and  $K_0$  represent the energy per nucleon and the incompressibility coefficient of SNM. The linear term is absent because the pressure

around the minimum energy  $\varepsilon_0$  are controlled by the incompressibility coefficient  $K_0$ . The corresponding quantities in the case of the symmetry energy are denoted by  $J$  and  $K_{\text{sym}}$ . However, unlike the case of symmetric nuclear matter, the slope of the symmetry energy  $L$  does not vanish at saturation density. Indeed, assuming the validity of Eq. (19),  $L$  is directly proportional to the pressure of pure neutron matter at saturation density:

$$P_0 \approx \frac{1}{3} \rho_0 L . \quad 21.$$

Hence, finding experimental observables that can effectively constrain the slope of the symmetry energy  $L$  is tantamount to the determination of the pressure of a cold neutron gas at saturation density. As we show in Sec.3, we will explore the predictions of several nuclear density functionals that while all successful in reproducing a host of laboratory observables, predict significant differences in the properties of neutron-rich systems, such as exotic nuclei and neutron stars.

### 3. RESULTS

This section is devoted to establish compelling connections between the properties of finite nuclei and neutron stars. To assess uncertainties in the density dependence of the symmetry energy we rely on a set of nine successful covariant energy density functionals. Among them, NL3(63, 102) and IU-FSU(68) have been used extensively in the literature. In particular, the IU-FSU functional represented an improvement over the original FSUGold model (66) by accounting for the existence of massive neutron stars (79, 80, 81). In addition, three different TAMU-FSU models, all with a relatively stiff symmetry energy, were introduced in Ref.(103) to explore whether existing experimental data could rule out thick neutron skins in  $^{208}\text{Pb}$ . The remaining density functionals were calibrated for the first time using exclusively physical observables (37, 69). That is, unlike earlier approaches, bulk properties of infinite nuclear matter were now predicted rather than assumed. Moreover, the calibration protocol relied on a statistically robust covariance analysis that provided both theoretical uncertainties and correlation coefficients (37). The only significant difference in the calibration of these functionals was an assumed value for the presently unknown neutron skin thickness of  $^{208}\text{Pb}$  (69).

#### 3.1. Ground State Properties

To assess the performance of the nine models employed in this work we display in Fig.1 theoretical predictions relative to experiment for the binding energies per nucleon (104) and charge radii (105) of a representative set of magic and semi-magic nuclei. In all cases the predictions fall within 2% of the experimental values. However, it is worth mentioning that for most of these functionals, the binding energies and charge radii displayed in the figure were incorporated into the fitting protocol. Nevertheless, these results suggest that extrapolations to the high density regime characteristic of neutron stars involve covariant EDFs that are consistent with known properties of finite nuclei.

#### 3.2. Neutron Star Properties

Although both relativistic and non-relativistic energy density functionals have been enor-

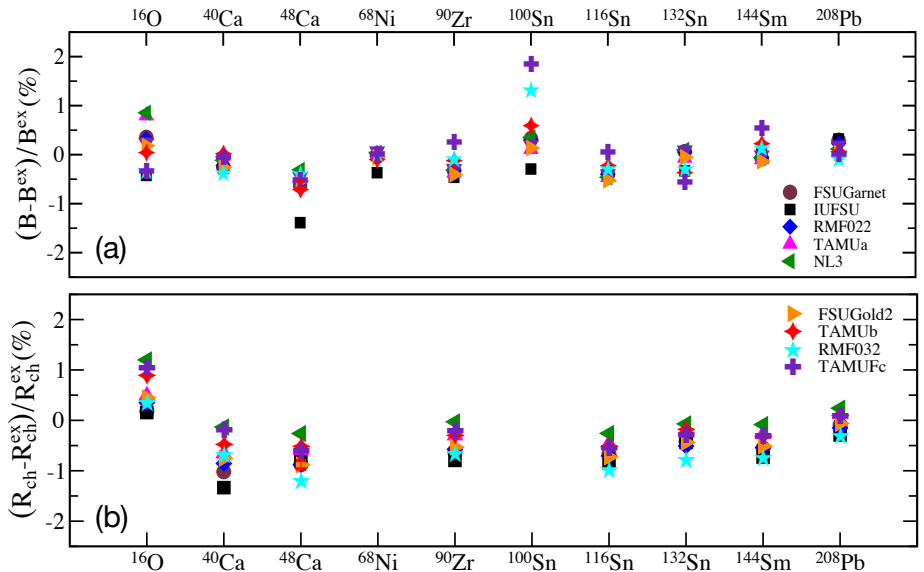


**Figure 1**

Comparison between the theoretical predictions of the nine models introduced in the text for (a) the binding energy and (b) charge radius of a representative set of magic and semi-magic nuclei. Results are shown as the fractional discrepancy in percent.

response, there is a distinct advantage in using a Lorentz covariant formulation as one extrapolates to dense nuclear matter. Inherent to any consistent relativistic framework is the observance of “causality”, namely, the fact that no signal can propagate faster than the speed of light. In the context of dense matter, this implies a limit to the stiffness of the equation of state given by  $P \leq \varepsilon$ , which in the context of Eq.(14) implies that the speed of sound remains below the speed of light at all densities. However, the causal limit is often violated in non-relativistic descriptions, especially as central densities become large enough to support  $2M_{\odot}$  neutron stars. Violating causality is particularly problematic in the case of the tidal polarizability as the relevant differential equation depends explicitly on the speed of sound; see Eq.(13b).

Predictions for the equation of state of symmetric nuclear matter and the symmetry energy are displayed in Fig.2. Under the assumption that Eq.(19) is valid, the EOS of pure neutron matter (not shown) is approximately equal to the sum of these two contributions. In the case of symmetric nuclear matter, all models predict a saturation point located at  $\rho_0 \approx 0.15 \text{ fm}^{-3}$  and a binding energy per nucleon of  $\varepsilon_0 \approx -16 \text{ MeV}$ . Note that we use “predict” as many of these functionals were calibrated using exclusively physical observables, namely, no bulk properties of nuclear-matter were incorporated into the calibration procedure (37, 69). This suggest that the values commonly adopted for both  $\rho_0$  and  $\varepsilon_0$  are properly encoded in certain bulk properties of finite nuclei.

Beyond the saturation point, the small oscillations around the minimum are controlled by the incompressibility coefficient  $K_0$ . Experimental measurements of the giant monopole resonance in  $^{208}\text{Pb}$ —and also on a few lighter nuclei such as  $^{144}\text{Sm}$  and  $^{90}\text{Zr}$ —have con-

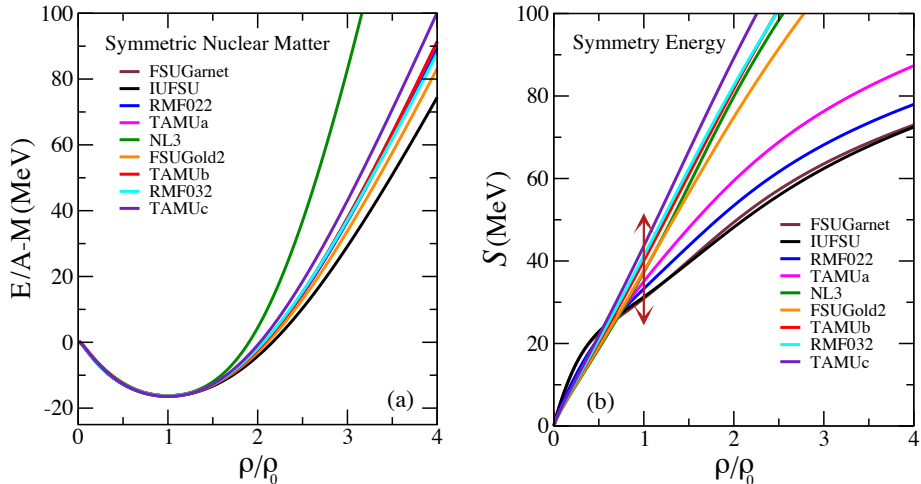


**Figure 2**

Binding energy per nucleon (a) and nuclear symmetry energy (b) as a function of the baryon density as predicted by the nine models described in the text. The arrow in (b) is indicative of the large model spread in the slope of the symmetry energy at saturation density.

and references contained therein. The NL3 model (shown in green) was conceived before such stringent constraints were available, leading to a large incompressibility coefficient  $K_0$  that, in turn, generates a very stiff EOS for symmetric nuclear matter. In contrast, some of the most recently-calibrated functionals have incorporated for the first time information on giant monopole energies. As such, the incompressibility coefficient predicted by these models is fully consistent with experiment (37). However, note that measurements of the distribution of isoscalar monopole strength in the isotopic chains of both tin and cadmium seem to suggest a smaller value for  $K_0$  (107, 108). After more than a decade, the issue of the softness (or “fluffiness”) of these open-shell nuclei remains unresolved (109, 110).

Whereas ground-state properties and collective excitations of finite nuclei impose stringent constraints on the behavior of symmetric nuclear matter, this is no longer true for the symmetry energy; see Fig.2(b). It appears that nuclear ground-state properties—particularly the masses of neutron-rich nuclei—determine rather accurately the value of the symmetry energy at about two thirds of nuclear matter saturation density, or at  $\rho \approx (2/3)\rho_0 \approx 0.1 \text{ fm}^{-3}$  (71, 95, 96, 111, 112). However, the slope of the symmetry energy in the vicinity of saturation density is poorly constrained by nuclear observables. In order to mitigate this problem, the neutron skin thickness of  $^{208}\text{Pb}$  was identified as an ideal proxy for  $L$ . Indeed, a very strong correlation was found between  $L$  and the neutron skin thickness of  $^{208}\text{Pb}$  (95, 96, 97, 98). Given that symmetric nuclear matter saturates, the slope of the symmetry energy  $L$  is directly related to the pressure of pure neutron matter at saturation density; see Eq.(21). As a result, a measurement of the neutron skin thickness of  $^{208}\text{Pb}$  provides critical information on a fundamental parameter of the equation of state. Motivated by this finding, the lead radius experiment (PREX) at JLab was commissioned about a decade ago and has already provided the first model-independent evidence in favor of a neutron-rich skin in  $^{208}\text{Pb}$  (113, 114). Unfortunately, due to unanticipated experimen-

neutron radius of  $^{208}\text{Pb}$ . Since then, the follow-up PREX-II campaign was successfully completed and the brand new Calcium Radius EXperiment (CREX) was commissioned at the time of this writing (6). In conjunction, PREX-II and CREX will provide valuable information on the equation of state of neutron-rich matter. Until then, one must explore how the uncertainties in the density dependence of the symmetry energy impact our predictions on the properties of neutron stars.

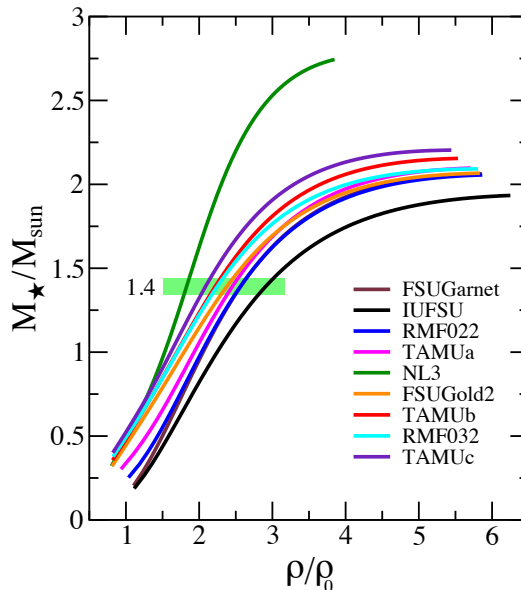


**Figure 3**

Relationship between the mass of a neutron star and the central density required to support such a star as predicted by the nine models described in the text. The green bar illustrates the significant model dependence in the central density required to support a  $1.4M_{\odot}$  neutron star.

Although PREX-II and CREX constrain the behavior of neutron-rich matter in the vicinity of nuclear matter saturation density, neutron stars are sensitive to the equation of state up to several times saturation density. To assess the range of densities probed in the interior of neutron stars we display in Fig.3 the central density required to support a neutron star of a given mass. As expected, the required central density depends critically on the stiffness of the equation of state. For example, in the case of NL3—the model with the stiffest EOS—the central density lies below  $4\rho_0$  for all masses below its predicted maximum mass of  $\sim 2.7M_{\odot}$ . In contrast, the IUFSU model with the softest EOS requires a central density in excess of  $6\rho_0$  to support a maximum mass of  $\lesssim 2M_{\odot}$ . Note that these densities may get even higher in the event of a phase transition in the stellar core—a situation that we do not contemplate in this contribution. Finally, the green bar in the figure illustrates the model dependence in the central density that is required to support a “canonical”  $1.4M_{\odot}$  neutron star: from less than twice  $\rho_0$  (for NL3) to about three times  $\rho_0$  for IUFSU.

Stellar radii, however, seem to be largely determined by the density dependence of the symmetry energy in the immediate vicinity of nuclear matter saturation density. Indeed,

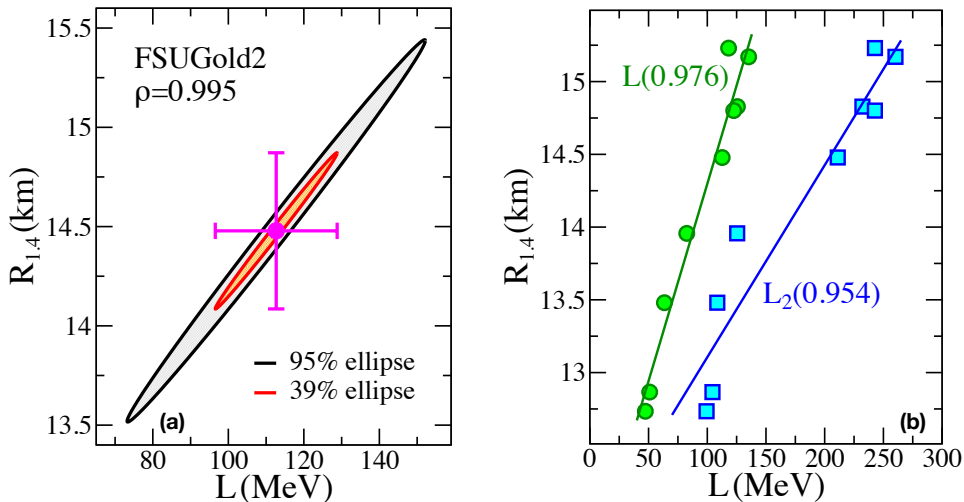


**Figure 4**

The 39% and 95% confidence ellipses between the slope of symmetry energy  $L$  and the radius of a  $1.4M_{\odot}$  neutron star as predicted by the FSUGold2 density functional (a). Also displayed in the figure are the corresponding statistical errors in  $L$  and  $R_{1.4}$ . Systematic uncertainties in the same correlation but now as predicted by the nine models described in the text (b). Also shown is the correlation between  $L_2$  (the slope of symmetry energy at twice saturation density) and  $R_{1.4}$ .

for stellar radii (94). This suggests that although PREX-II can not determine the stiffness of the EOS at high densities, it should provide valuable insights into the overall size of neutron stars (71, 73). To underscore the strong correlation between the slope of the symmetry energy  $L$  and the radius of a  $1.4M_{\odot}$  neutron star we display in Fig. 4(a) 39% and 95% confidence ellipses using the FSUGold2 density functional as an example. FSUGold2 is particularly convenient to illustrate this correlation as no biases were introduced in the calibration of the functional—particularly in connection to the (presently unknown) neutron skin thickness of  $^{208}\text{Pb}$  (37). With a correlation coefficient of almost one ( $\rho = 0.995$ ) and nearly “degenerate” ellipses, a nearly one-to-one correspondence exists between  $L$  and  $R_{1.4}$ . Given that the neutron skin thickness of  $^{208}\text{Pb}$  provides an ideal proxy for  $L$ , a powerful “data-to-data” relation emerges between neutron-rich systems—finite nuclei and neutron stars—that differ in size by 18 orders of magnitude.

Although the correlation displayed in Fig. 4(a) is compelling, the statistical analysis carried out is unable to assess *systematic* errors associated to the intrinsic limitations of a given model; in this case FSUGold2. In order to properly assess systematic uncertainties, we include in Fig. 4(b) the predictions of each of the nine models considered in the text. Although slightly weaker ( $\rho = 0.976$ ) than in Fig. 4(a), the correlation between  $L$  and  $R_{1.4}$  remains very strong. Note, however, that the correlation between  $R_{1.4}$  and the slope of the symmetry energy at *twice* saturation density ( $L_2$ ) appears slightly weaker. In light of the expectation that stellar radii are sensitive to the density dependence of the symmetry energy near twice saturation density (94), our finding is mildly surprising, so it should be examined within the context of a more diverse set of energy density functionals.



is displayed on Fig.5(b). In addition to these nine theoretical predictions the figure includes several interesting limits. The 1939 prediction by Oppenheimer and Volkoff for the maximum neutron star mass—assuming that the entire pressure support is due to a non-interacting Fermi gas of neutrons—is displayed in the lower part of the figure (76). This pioneering prediction has long been refuted, especially with the confirmation of three neutron stars with masses in the vicinity of  $2M_{\odot}$  (79, 80, 81); see the three bars in the upper portion of the figure. In particular, Cromartie and collaborators have measured a neutron star with a mass of about  $2.14M_{\odot}$  (81)—a value that is tantalizingly close to the *upper limit* of  $M_{\max} = 2.17M_{\odot}$  suggested by Margalit and Metzger from exploiting the multimessenger nature of GW170817 (84). By also combining gravitational-wave and electromagnetic information from GW170817, Bauswein and collaborators provided a *lower limit* on the radius of a  $1.6M_{\odot}$  neutron star (43) which, when combined with the upper limits obtained in Refs. (44, 45), results in the two arrows facing each other in the figure. Finally, the figure includes results from the very recent (few days old!) simultaneous extraction of the mass and radius of PSR J0030+0451 by the Neutron Star Interior Composition Explorer (NICER). The quoted results by Miller and collaborators are:  $M = 1.44^{+0.15}_{-0.14}M_{\odot}$  and  $R = 13.02^{+1.24}_{-1.06}M_{\odot}$  (118). These values are consistent with the independent analysis reported by Riley and collaborators in Ref. (119). Although the first NICER results do not impose stringent constraints on the EOS, this pioneering measurement determined for the first time the gravitational mass and equatorial radius of a neutron star.

So what do we conclude? On the one hand, the existence of massive neutron stars suggests that the EOS at high densities must be relatively stiff to provide the necessary pressure support. On the other hand, GW170817 seems to favor compact stars with small radii—suggesting instead that the EOS must be soft. How can we then simultaneously account for both small radii and large masses? As argued earlier, stellar radii appear to be sensitive to the EOS of neutron-rich matter in the vicinity of nuclear matter saturation density. In contrast, the maximum neutron star mass is sensitive to the equation of state at the highest densities attained in the stellar core. Hence, the apparent tension may be resolved if the EOS is soft at intermediate densities—thereby accounting for the small radii—but then stiffens at higher densities in order to support heavy neutron stars. This already unique situation could become even more interesting if PREX-II confirms the original PREX measurement of a neutron skin thickness of  $R_{\text{skin}}^{208} = 0.33$  fm, albeit with larger error bars (113, 114). If confirmed, this would imply that the EOS is stiff in the vicinity of saturation density, it will then soften at intermediate densities to account for the small stellar radii, but will ultimately stiffen at high densities to explain the existence of massive neutron stars. The evolution from stiff to soft and back to stiff may reflect a fascinating underlying dynamics, perhaps indicative of an exotic phase transition in the stellar interior.

## 4. CONCLUSIONS

Nuclear science is driven by the quest to understand the fundamental interactions that shape the structure of the universe. A new generation of terrestrial facilities being commissioned all over the world will help answer some key science questions, such as *How did visible matter come into being and how does it evolve?* and *How does subatomic matter organize itself and what phenomena emerge?* (1). Insights into the dynamics of neutron-rich matter will emerge as one probes exotic nuclei with very large neutron skins. In the cosmos, neutron-rich matter is produced in the cores of massive stars and in the aftermath of their collapse. What is the

*states of matter at exceedingly high density and temperature?* and *How were the elements from iron to uranium made?* (120). Remarkable development within the last few years—and in some cases during the past few months—are providing valuable insights into the nature of dense neutron-rich matter. First, the direct detection of gravitational waves from the binary neutron star merger GW170817 suggests that neutron stars are fairly compact, implying a relatively soft EOS at intermediate densities (38). Second, the observation by Cromartie and collaborators of the most massive neutron star to date implies that the EOS must stiffen at high densities (81). Finally, NICER—aboard the international space station—reported the very first simultaneous measurement of the mass and radius of a neutron star (118, 119). This pioneering result is highly significant as a one-to-one correspondence exists between the mass-radius relation of neutron stars and the underlying equation of state (121).

As we embark on this new journey of discovery, nuclear theory will play a critical role in guiding new experimental programs. As critical, nuclear theory will continue to make predictions in regimes that will remain inaccessible to experiment and observation. Prospects in nuclear theory are excellent given the recent advances in ab initio methods that start from chiral EFT Hamiltonians fitted to two- and three-body data (8). Indeed, within the last decade ab initio calculations have seen an explosive growth in scalability to larger systems. Yet despite this undeniable progress, density functional theory remains the most promising and only tractable approach that may be applied over the entire nuclear landscape: from finite nuclei to neutron stars. It was the main goal of this review to demonstrate the power and flexibility of modern covariant energy density functionals in predicting the properties of nuclear system across such a rich and diverse landscape. Particularly important in this context is the unique synergy between nuclear physics and astrophysics in the brand new era of gravitational wave astronomy.

So what is the path forward in the development of density functional theory as it pertains to nuclear physics? Perhaps the most serious obstacle is the lack of a one-to-one correspondence between the one-body nuclear density and a suitable external potential, a requirement that is germane to DFT as originally conceived by Hohenberg and Kohn (9, 10). Moreover, unlike DFT applications to electronic structure where the fundamental interaction is known, the underlying nucleon-nucleon interaction—although often inspired by QCD—relies on fits to two- and three-nucleon data. A much more fruitful application of DFT to nuclear physics is through the Kohn-Sham equations, a set of equations that are highly reminiscent of the traditional mean-field approach that lies at the heart of nuclear physics. However, in contrast to the Kohn-Sham formalism that yields in principle the exact ground-state energy and one-body density, no such guarantee exists in nuclear physics since the “universal” nuclear mean-field potential is unknown. Nevertheless, enormous progress in ab initio approaches provide meaningful benchmarks for the refinement of existing nuclear functionals. The CREX campaign at JLab was motivated in part by the powerful connection between ab initio approaches and DFT (6, 7). Finally, nuclear density functionals will be informed and refined by the wealth of experimental and observational data that will emerge from rare isotope facilities, telescopes operating across the entire electromagnetic spectrum, and ever more sensitive gravitational wave detectors. This unique synergy will prove vital in our quest to determine the nuclear equation of state.

## ACKNOWLEDGMENTS

This material is based upon work supported by the U.S. Department of Energy Office of Science, Office of Nuclear Physics under Award Number DE-FG02-92ER40750.

## LITERATURE CITED

1. Geesaman D, et al. Reaching for the Horizon; The 2015 Long Range Plan for Nuclear Science
2. Pieper SC, Wiringa RB. *Ann. Rev. Nucl. Part. Sci.* 51:53 (2001)
3. Barrett BR, Navratil P, Vary JP. *Prog. Part. Nucl. Phys.* 69:131 (2013)
4. Hagen G, Papenbrock T, Hjorth-Jensen M, Dean DJ. *Rept. Prog. Phys.* 77:096302 (2014)
5. Navratil P, et al. *Phys. Scripta* 91:053002 (2016)
6. Mammei J, et al. CREX: Parity-violating measurement of the weak-charge distribution of  $^{48}\text{Ca}$  (2013)
7. Horowitz CJ, Kumar KS, Michaels R. *Eur. Phys. J.* A50:48 (2014)
8. Furnstahl RJ arXiv:1906.00833 [nucl-th] (2019)
9. Hohenberg P, Kohn W. *Phys. Rev.* 136:B864 (1964)
10. Kohn W, Sham LJ. *Phys. Rev.* 140:A1133 (1965)
11. Kohn W. *Rev. Mod. Phys.* 71:1253 (1999)
12. Fiolhais C, Nogueira F, Marques M (2003). A Primer in Density Functional Theory. Springer-Verlag
13. Burke K. The ABC of DFT; <http://chem.ps.uci.edu/kieron/dft/book/> (2007)
14. Skylaris CK. DFT Lectures <https://www.southampton.ac.uk/compchem/people/teaching.page/>
15. Drut JE, Furnstahl RJ, Platter L. *Prog. Part. Nucl. Phys.* 64:120 (2010)
16. Negele JW. *Rev. Mod. Phys.* 54:913 (1982)
17. Skyrme THR. *Phil. Mag.* 1:1043 (1956)
18. Skyrme T. *Nucl. Phys.* 9:615 (1959)
19. Vautherin D, Brink DM. *Phys. Rev.* C5:626 (1972)
20. Stone JR, Reinhard PG. *Prog. Part. Nucl. Phys.* 58:587 (2007)
21. Bertsch GF. *Journal of Physics: Conference Series* 78:012005 (2007)
22. Stoitsov M, et al. *Journal of Physics: Conference Series* 180:012082 (2009)
23. Kortelainen M, et al. *Phys.Rev.* C82:024313 (2010)
24. Erler J, et al. *Nature* 486:509 (2012)
25. Kortelainen M, et al. *Phys. Rev. C* 89:054314 (2013)
26. Thouless D. *Nuclear Physics* 22:78 (1961)
27. Dawson JF, Furnstahl RJ. *Phys. Rev.* C42:2009 (1990)
28. Piekarewicz J. *Phys. Rev.* C64 (2001)
29. Ring P, Schuck P (2004). The Nuclear Many-Body Problem. Springer, New York
30. Fattoyev F, Piekarewicz J. *Phys. Rev.* C84:064302 (2011)
31. Reinhard PG, Nazarewicz W. *Phys. Rev.* C81:051303 (2010)
32. Fattoyev F, Piekarewicz J. *Phys. Rev.* C88 (2012)
33. Reinhard P, Nazarewicz W. *Phys. Rev.* C87:014324 (2013)
34. Reinhard PG, et al. *Phys.Rev.* C88:034325 (2013)
35. Dobaczewski J, Nazarewicz W, Reinhard PG. *J. Phys.* G41:074001 (2014)
36. Piekarewicz J, Chen WC, Fattoyev F. *J. Phys.* G42:034018 (2015)
37. Chen WC, Piekarewicz J. *Phys. Rev.* C90:044305 (2014)
38. Abbott BP, et al. *Phys. Rev. Lett.* 119:161101 (2017)
39. Drout MR, et al. *Science* 358:1570 (2017)
40. Cowperthwaite PS, et al. *Astrophys. J.* 848:L17 (2017)
41. Chornock R, et al. *Astrophys. J.* 848:L19 (2017)

43. Bauswein A, Just O, Janka HT, Stergioulas N. *Astrophys. J.* 850:L34 (2017)
44. Fattoyev FJ, Piekarewicz J, Horowitz CJ. *Phys. Rev. Lett.* 120:172702 (2018)
45. Annala E, Gorda T, Kurkela A, Vuorinen A. *Phys. Rev. Lett.* 120:172703 (2018)
46. Abbott BP, et al. *Phys. Rev. Lett.* 121:161101 (2018)
47. Most ER, Weih LR, Rezzolla L, Schaffner-Bielich J. *Phys. Rev. Lett.* 120:261103 (2018)
48. Tews I, Margueron J, Reddy S. *Phys. Rev.* C98:045804 (2018)
49. Malik T, et al. *Phys. Rev.* C98:035804 (2018)
50. Tsang CY, et al. arXiv:1807.06571 [nucl-ex] (2018)
51. Radice D, Dai L arXiv:1810.12917 [astro-ph.HE] (2018)
52. Piekarewicz J. *Eur. Phys. J. A* 50:25 (2013)
53. Piekarewicz J. *Int. J. Mod. Phys.* E24:1541003 (2015)
54. Bender M, Heenen PH, Reinhard PG. *Rev.Mod.Phys.* 75:121 (2003)
55. Johnson MH, Teller E. *Phys. Rev.* 98:783 (1955)
56. Duerr HP. *Phys. Rev.* 103:469 (1956)
57. Miller LD, Green AES. *Phys. Rev.* C5:241 (1972)
58. Serot BD, Walecka JD. *Adv. Nucl. Phys.* 16:1 (1986)
59. Walecka JD. *Annals Phys.* 83:491 (1974)
60. Youngblood DH, et al. *Phys. Rev. Lett.* 39:1188 (1977)
61. Boguta J, Bodmer AR. *Nucl. Phys.* A292:413 (1977)
62. Mueller H, Serot BD. *Nucl. Phys.* A606:508 (1996)
63. Lalazissis GA, Konig J, Ring P. *Phys. Rev.* C55:540 (1997)
64. Vretenar D, Niksic T, Ring P. *Phys. Rev.* C68:024310 (2003)
65. Lalazissis GA, Niksic T, Vretenar D, Ring P. *Phys. Rev.* C71:024312 (2005)
66. Todd-Rutel BG, Piekarewicz J. *Phys. Rev. Lett* 95:122501 (2005)
67. Agrawal B. *Phys.Rev.* C81:034323 (2010)
68. Fattoyev FJ, Horowitz CJ, Piekarewicz J, Shen G. *Phys. Rev.* C82:055803 (2010)
69. Chen WC, Piekarewicz J. *Phys. Lett.* B748:284 (2015)
70. Serot BD, Walecka JD. *Int. J. Mod. Phys.* E6:515 (1997)
71. Horowitz CJ, Piekarewicz J. *Phys. Rev. Lett.* 86:5647 (2001)
72. Todd BG, Piekarewicz J. *Phys. Rev.* C67:044317 (2003)
73. Horowitz CJ, Piekarewicz J. *Phys. Rev.* C64:062802 (2001)
74. Carriere J, Horowitz CJ, Piekarewicz J. *Astrophys. J.* 593:463 (2003)
75. Tolman RC. *Phys. Rev.* 55:364 (1939)
76. Oppenheimer JR, Volkoff GM. *Phys. Rev.* 55:374 (1939)
77. Thorsett S, Chakrabarty D. *Astrophys. J.* 512:288 (1999)
78. Lattimer JM, Prakash M. *Science* 304:536 (2004)
79. Demorest P, et al. *Nature* 467:1081 (2010)
80. Antoniadis J, et al. *Science* 340:6131 (2013)
81. Cromartie HT, et al. arXiv:1904.06759 [astro-ph.HE] (2019)
82. Chandrasekhar S. *Astrophys. J* 74:81 (1931)
83. Weinberg S (1972). *Gravitation and Cosmology.* John Wiley & Sons, New York
84. Margalit B, Metzger BD. *Astrophys. J.* 850:L19 (2017)
85. Binnington T, Poisson E. *Phys. Rev.* D80:084018 (2009)
86. Damour T, Nagar A, Villain L. *Phys. Rev.* D85:123007 (2012)
87. Hinderer T. *Astrophys. J.* 677:1216 (2008)
88. Hinderer T, Lackey BD, Lang RN, Read JS. *Phys. Rev.* D81:123016 (2010)
89. Damour T, Nagar A. *Phys. Rev.* D80:084035 (2009)
90. Postnikov S, Prakash M, Lattimer JM. *Phys. Rev.* D82:024016 (2010)
91. Fattoyev FJ, Carvajal J, Newton WG, Li BA. *Phys. Rev.* C87:015806 (2013)
92. Steiner AW, Gandolfi S, Fattoyev FJ, Newton WG. *Phys. Rev.* C91:015804 (2015)
93. Piekarewicz J, Fattoyev FJ. *Phys. Rev.* C99:045802 (2019)

94. Lattimer JM, Prakash M. *Phys. Rept.* 442:109 (2007)
95. Brown BA. *Phys. Rev. Lett.* 85:5296 (2000)
96. Furnstahl RJ. *Nucl. Phys.* A706:85 (2002)
97. Centelles M, Roca-Maza X, Viñas X, Warda M. *Phys. Rev. Lett.* 102:122502 (2009)
98. Roca-Maza X, Centelles M, Viñas X, Warda M. *Phys. Rev. Lett.* 106:252501 (2011)
99. Page D, Reddy S. *Ann. Rev. Nucl. Part. Sci.* 56:327 (2006)
100. Piekarewicz J (2017). in *Neutron Star Matter Equation of State*. Cham: Springer International Publishing
101. Piekarewicz J, Centelles M. *Phys. Rev.* C79:054311 (2009)
102. Lalazissis GA, Raman S, Ring P. *At. Data Nucl. Data Tables* 71:1 (1999)
103. Fattoyev FJ, Piekarewicz J. *Phys. Rev. Lett.* 111:162501 (2013)
104. Huang WJ, et al. *Chin. Phys.* C41:030002 (2017)
105. Angeli I, Marinova K. *At. Data Nucl. Data Tables* 99:69 (2013)
106. Garg U, Coló G. *Prog. Part. Nucl. Phys.* 101:55 (2018)
107. Li T, et al. *Phys. Rev. Lett.* 99:162503 (2007)
108. Patel D, et al. *Phys. Lett.* B718:447 (2012)
109. Garg U, et al. *Nucl. Phys.* A788:36 (2007)
110. Piekarewicz J. *Phys. Rev.* C76:031301 (2007)
111. Ducoin C, Margueron J, Providencia C, Vidana I. *Phys. Rev.* C83:045810 (2011)
112. Horowitz CJ, et al. *J. Phys.* G41:093001 (2014)
113. Abrahamyan S, et al. *Phys. Rev. Lett.* 108:112502 (2012)
114. Horowitz CJ, et al. *Phys. Rev.* C85:032501 (2012)
115. Abbott BP, et al. *Phys. Rev. Lett.* 116:061102 (2016)
116. Thiel M, et al. *J. Phys.* G46:093003 (2019)
117. Piekarewicz J, Fattoyev FJ. *Physics Today* 72:30 (2019)
118. Miller MC, et al. *Astrophys. J. Lett.* 887:L24 (2019)
119. Riley TE, et al. *Astrophys. J. Lett.* 887:L21 (2019)
120. Turner MS, et al. (2003). *Connecting Quarks with the Cosmos: Eleven Science Questions for the New Century*. Washington, DC: The National Academies Press
121. Lindblom L. *Astrophys. J.* 398:569 (1992)